BL5U

Interfacing 2D and 3D Topological Insulators: Bi(111) Bilayer on Bi$_2$Te$_3$

T. Hirahara[1], G. Bihlamyer[2], Y. Sakamoto[1], M. Yamada[1], H. Miyazaki[3], S. Kimura[3],
S. Blügel[2] and S. Hasegawa[1]

[1]*Department of Physics, University of Tokyo, 7-3-1 Hongo, Bunkyo-ku, Tokyo 113-0033, Japan*
[2]*Peter Grünberg Institut and Institute for Advanced Simulation, Forschungszentrum Jülich and JARA, 52425 Jülich, Germany*
[3]*UVSOR Facility, Institute for Molecular Science, Okazaki 444-8585, Japan*

Topological insulators (TI) are a novel state of quantum matter in three dimensions (3D) that have been gaining increased attention. Along with its two-dimensional (2D) counterpart, the quantum spin Hall (QSH) phase, they are mathematically characterized by the so-called Z_2 topological number [1]. While the bulk is insulating with an inverted gap, there is a metallic edge or surface state which is topologically protected and hence robust against weak perturbation or disorder.

While there have been a large number of reports on 3D TI, only few works have been done in terms of 2D QSH. The most extensively studied system is the HgTe/CdTe quantum well [2]. Another important system predicted to be a 2D QSH is the single bilayer (BL) Bi [3]. But since it is the thinnest limit for a 2D system similar to graphene, it has not been realized experimentally.

In the present research, we succeeded in fabricating a single bilayer of Bi(111) on Bi$_2$Te$_3$(111) since they both form in layers with a hexagonal lattice. We have investigated how the surface Dirac cone of Bi$_2$Te$_3$ is affected by this Bi termination. Figures 1 (a) and (b) show the band dispersion for the 18 QL (quintuple layer, stack of Te-Bi-Te-Bi-Te) Bi$_2$Te$_3$(111) film on silicon and a bilayer of Bi(111) on top of it, respectively, measured by angle-resolved photo-emission spectroscopy. The Dirac cone as well as the bulk conduction/valence bands can be seen in Fig. 1(a). We should note that due to the overlap of the bulk valence band and the Dirac cone near the Dirac point, the photoemission intensity is strongly suppressed near the Γ point. The Dirac cone does not vanish upon Bi adsorption as can be clearly seen in Fig. 1(b), which is a direct evidence that the the Dirac cone is actually robust against nonmagnetic perturbations. However, the intensity at the Dirac point is enhanced and it seems that the Dirac cone has changed its nature. Comparison of the present experimental data with *ab initio* calculations showed that the electronic structure of the Bi/Bi$_2$Te$_3$ system can be understood as an overlap of the band dispersions of bilayer Bi and Bi$_2$Te$_3$. But whereas the Dirac cone of Bi$_2$Te$_3$ is localized at the topmost QL, the Dirac cone in Fig. 1(b) was mostly localized at the topmost Bi and this change induced the change in the experimental observation. Our results show a unique situation where the topologically protected one- and two-dimensional edge states are coexisting at the surface [4].
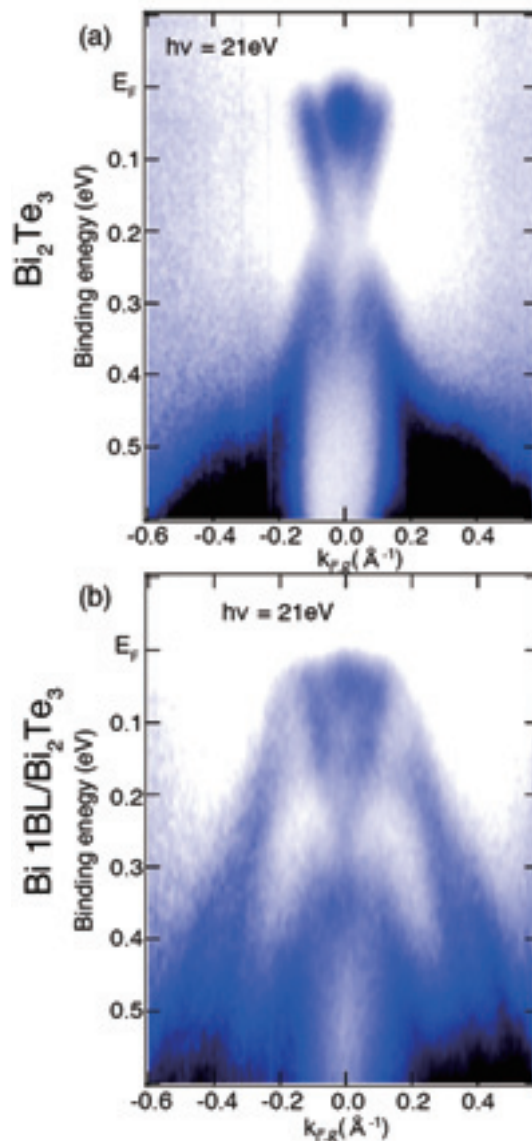

Fig. 1. Band dispersion image of a 18 QL thick Bi$_2$Te$_3$ (a), and that for a single-bilayer Bi(111) terminated Bi$_2$Te$_3$ (b).

[1] M. Z. Hasan and C. L. Kane, Rev. Mod. Phys. **82** (2010) 3045.
[2] M. König *et al.,* Science **318** (2007) 766.
[3] S. Murakami, Phys. Rev. Lett. **97** (2006) 236805.
[4] T. Hirahara *et al.,* Phys. Rev. Lett. **107** (2011) 166801.

III-4. SURFACE AND THIN FILMS

Polarized NEXAFS Study on Nitrogen Dopant in Rutile TiO$_2$(110)

Y. Monya[1], M. Nagasaka[2], H. Yamane[2], N. Kosugi[2] and H. Kondoh[1]

[1]*Graduate School of Science and Technology, Keio University, Yokohama 223-8522, Japan*
[2]*Institute for Molecular Science, Okazaki 444-8585, Japan*

Nitrogen doped TiO$_2$, which is one of most promising visible-light-response photocatalysts, has been extensively studied to understand the mechanism of visible-light-response. Although many structural studies on nitrogen dopants in TiO$_2$ have been conducted with various techniques, neither site nor chemical state of the nitrogen dopant is clear yet. In this work, we measured polarized NEXAFS spectra for nitrogen-doped rutile TiO$_2$(110) to elucidate the structure of the nitrogen dopants.

The samples were prepared by heating TiO$_2$(110) substrates under NH$_3$ atmosphere. Polarized NEXAFS experiments were performed at BL3U with using the partial electron yield method.

Figure 1 shows O-K edge NEXAFS spectra of rutile TiO$_2$(110) with different polarization angles. For example, NI [001] indicates that x-ray incidence angle is 90° from the surface parallel and its electric vector is lying along [001] direction (see Fig. 2). In the grazing incidence (GI) geometry, the incidence angle was 30°. For the O-K NEXAFS spectra, we observe seven peaks (a-g) depending on the polarization. Considering the polarization dependence and previous assignments for these peaks [1,2], peaks a, b and d can be attributed to excitations to three unoccupied states: (Ti 3d + O 2pπ), (Ti 3d + O 2pσ) and (Ti 4s + O 2p), respectively. Peaks e and f are assigned to (Ti 4p + O 2pπ and σ). Peaks c and g seem to be associated with of a surface oxygen species shown in Fig. 2. The peak c is attributed to the combination of Ti 3d orbital and O 2p orbital of the surface oxygen species bridging two titanium atoms. Similarly, Peak g is attributed to the combination of Ti 4sp orbitals and O 2p orbital of the same oxygen species.

Figure 3 shows N-K edge NEXAFS spectra of the nitrogen dopants in the rutile TiO$_2$(110). Here the incidence angle was 15° for GI and 90° for NI. As a result, seven peaks (a'-f' and X) were observed and the peaks a'-f' well correspond to a-f in the O-K NEXAFS with respect to both polarization dependence and the order in energy. The counterpart of peak g is not clearly discernible due to a poor S/N ratio. From these results, the nitrogen dopants in rutile TiO$_2$ are likely to occupy the lattice oxygen sites via substitution.

It should be noted that peak X appears exclusive in the N-K edge spectra. Based on the results of XPS measured at BL6U and a previous report [3], it is proposed that the nitrogen dopants are in the form of NH. Thus, peak X might be attributed to an excitation to a NH-relating unoccupied orbital. The fact that peak X is enhanced in the GI geometry suggests that the N-H bond is aligned closely along the surface normal.
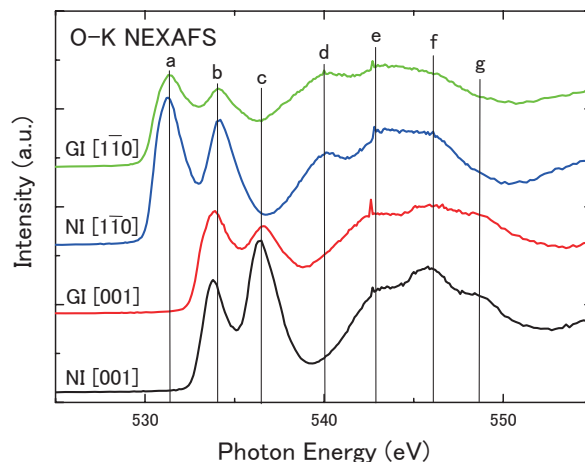

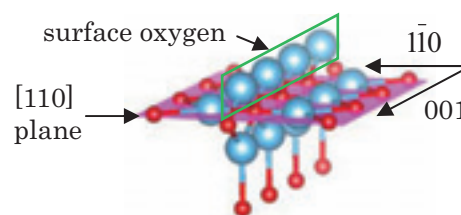Fig. 1. O-K NEXAFS spectra of rutile TiO$_2$(110).

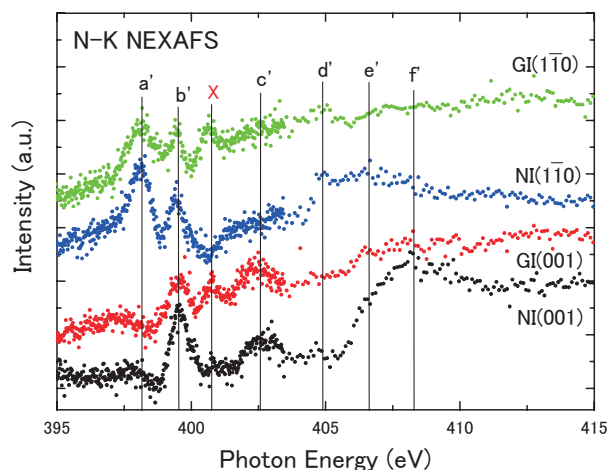Fig. 2. Rutile TiO$_2$(110) surface (K. Momma et al., J. Appl. Crystallogr. **44** (2011) 1272.)

Fig. 3. N-K NEXAFS spectra of nitrogen dopant in rutile TiO$_2$(110) .

[1] J. G. Chen, Surface Science Reports **30** (1997) 1.
[2] E. Filatova *et al.*, Phys. Status Solidi B **246** (2009) No.7, 1454.
[3] Y. Kim *et al.*, J. Phys. Chem. C **115** (2011) 18618.

Ⅲ-4. SURFACE AND THIN FILMS

BL3B

Photoionization of Polyaromatic Molecules on the Surface of Ionic Liquids

T. Ishioka, K. Tomita, Y. Imanishi, S. Furukawa and A. Harata

Department of Molecular and Material Sciences, Kyushu University, Kasuga-shi, Fukuoka 816-8580, Japan

Ionic liquids are rapidly expanding topics of research because of their fovorable properties such as high ionic conductivity, negligible vapor pressure, and controllable hydrophobicity. Much effort has been made to understand the unique physical properties of ionic liquids. The dielectric constant is one of them because many theoretical approaches rely on dielectric continuum models.

Recently, some authors reported on bulk dielectric constants of various ionic liquids [1, 2]. However, interfacial property is also important to understand the characteristics of ionic liquid since that is related to many applications such as solvent extraction and batteries. Until now little is known on the interfacial dielectric properties of ionic liquids. Photoionization is a suitable technique for studying interfacial dielectric state because given threshold reflects the solvation energy at the surface. In this report, ionization threshold energies of polyaromotic molecules on various ionic liquids were measured and interfacial properties of ionic liquids are discussed.

Ionic liquids used: 1-butyl-3-methylimidazolium tetrafluoroborate, hexafluorophosphate ([bmim][BF$_4$] and [bmim][PF$_6$]), ethylammonium nitrate, and protonated betain bistrifluoromethane sulfonylimide ([Hbet][Tf$_2$N]) were synthesized as a usual method. Pure water and formamide was used as reference solvents. In a typical photoionization measurement, the light was emitted from the chamber to a He-purged cell through an MgF$_2$ window. The range of light energy was in 4-8 eV. The emitted light was reflected with an Al mirror and vertically irradiated on the sample surface. High voltage (400V) was applied between the mesh electrode that was 5 mm above the liquid surface and a Pt cell with 25 mm in diameter. Hexane solutions of aromatic molecules (naphthacene, perylene, pyrene) were prepared at the concentration of 10^{-4} M and added dropwisely on the surface of ionic liquids by 200 µL. After evaporation of hexane, the photoinduced current ($\sim$ 0.1 pA) was measured by a picoammeter (Keithley model 428).

Measured photoionization spectra were analyzed and threshold values were determined by fitting the spectra to the empirical formula of $I = (E - E_{th})^{2.5}$. Figure 1 shows the obtained photoionization threshold plotted against $(1-1/\varepsilon)$, where ε is the relative permittibity of the liquid. The threshold energy lies higher in a vacuum for each aromatic carbon (naphthacene: 6.97 eV; perylene: 6.96 eV; pyrene: 7.43 eV) than in any other solvents because the threshold energy (E_{th}) satisfy the formula in the case of emitting electron into the air,

$E_{th} = I_p + P^+$ and P^+ where I_p and P^+ are the

ionization potential and polarization energy of the photoionized molecule, respectively and P^+ is always negative since the polarization is exothermic.
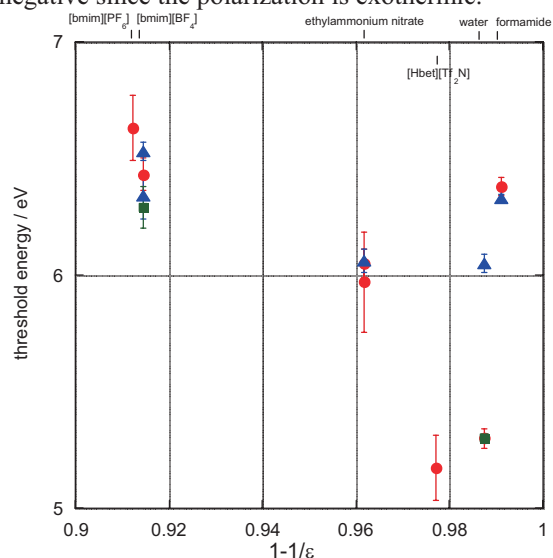

Fig. 1. Measured photoionization threshold plotted against a function of relative permitivity of each solvent. Round, triangle, and square plots are the results for perylene, pyrene, and naphtacene, respectively. Error bars are standard deviation for the measurement (n = 5).

Using Born's theory and making an assumption that each ionized molecule is spherically coordinated by surrounding solvent molecules, the polarization energy has a linear relationship with the value $(1-1/\varepsilon)$. However, for some polyaromatic molecules and solvents, the linearity cannot be applied and the absolute polarization energy is far smaller than the value estimated by complete solvation. The result imply that surface polyaromatic molecule is not fully solvated by surrounding ionic liquids. Furthermore, the photoionization threshold of pyrene shows the weakest dependence on the changes of bulk relative permittibity. This result coinsides with our previous report using ionic liquid/water mixture [3] where the photoionization threshold of pyrene has a small dependence on solvent composition. The analysis of the different behavior of polyaromatic molecules at the ionic liquid surfaces are now in progress.

[1] C. Wakai *et al.*, J. Phys. Chem. B **109** (2005) 17028.
[2] I. Krossing *et al.*, J. Am. Chem. Soc. **128** (2006) 13427.
[3] T. Ishioka, N. Inoue and A. Harata, UVSOR Activity Report **36** (2009) 58.

Ⅲ-4. SURFACE AND THIN FILMS

Huge Magnetic Anisotropy and Coercivity on Fe/W(110)

T. Nakagawa[1, 2], Y. Takagi[1, 2] and T. Yokoyama[1, 2]

[1]*Institute for Molecular Science, Okazaki 444-8585, Japan*
[2]*School of Physical Sciences, The Graduate University for Advanced Studies (SOKENDAI), Okazaki 444-8585, Japan*

Magnetic nanostructures have been an important subject both for application and fundamental researches. Materials with large coercivity and magnetic anisotropy are highly demanded for industrial uses. Single atomic layers, where magnetic features such as anisotropy, coercivity diverse from its bulk materials, give rise to extraordinary magnetic properties. Among magnetic single layers, Fe/W(110) has been one of the most extensively studied systems owing to its pseudomorphic growth mode, which results in 1x1 registry despite their large lattice mismatch ($a_{(W)}/a_{(Fe)} \sim 1.1$). The large expansion of Fe lattice has been inferred to generate a large magnetic anisotropy. However, due to its extremely large value, the anisotropy energy has not been directly determined in spite of huge accumulation of experimental results on Fe/W(110) [1].

We have investigated magnetic anisotropy energy and coercivity of Fe nanoislands on W(110) (Fig.1(a)) using x-ray circular dichroism (XMCD). The experiment was done at BL4B using a low temperature cryostat and a split pair superconductive magnet. The spectra were taken at T_s = 5K under magnetic field up to 6 T. The samples were prepared *in situ* with thermal deposition of Fe onto W single crystals.

Figure 1 (b) shows magnetization curves taken along three directions (see Fig.1 (c) for the configurations) by measuring the Fe L_3-edge white-line intensity. Using a first order anisotropy formula, $f(\theta,\phi)=c_1\cos^2\theta +c_2\sin^2\theta \sin^2 \phi–M$, we fits the magnetization curves. c_1 and c_2 are the magnetization anisotropy energies for [110] (out-of-plane) and [001] (in-plane) directions, respectively. The obtained anisotropy constants are plotted in Fig. 1 (d). The anisotropy energy is ~1 meV per Fe atom for the in-plane and out-of-plane directions as determined from magnetization curves, almost constant for the nanoisland below one monolayer. This anisotropy energy corresponds to an anisotropy field of 17 T. The coercivity, H_c, for the nanoislands at 0.25 ML is very large, ~5 T. With increasing the Fe coverage, giving larger island size, it rapidly decreases to 1 T at 0.6 ML, which follows $H_c \sim 1/r$ (radius of island).

The obtained largest coercivity is 1/3 of the anisotropy field, suggesting that the magnetization reversal process is via a domain wall creation, not a coherent rotation. In case of the coherent rotation at low temperature (~5 K), the coercivity should be close to the anisotropy energy.

Coercivity is limited by the smaller anisotropy energy since the magnetization reversal proceeds along the lower energy potential. Therefore, the large anisotropy both for the in-plane and out-of-plane directions is the origin of the huge coercivity on Fe/W(110).

[1] M. Pratzer, *et al*., Phys. Rev. Lett. **87** (2001) 127201.

Fig. 1. (a) Scanning tunneling microscopy image of Fe 0.3 ML deposited on W(110). (b) Magnetization curves on 0.4 ML Fe/W(110) for three directions (see (c)). (c) Experimental configurations for the XMCD measurements. (d) Anisotropy energies constant, c_1 and c_2 (see text) and (e) coercivity as a function of Fe coverage.
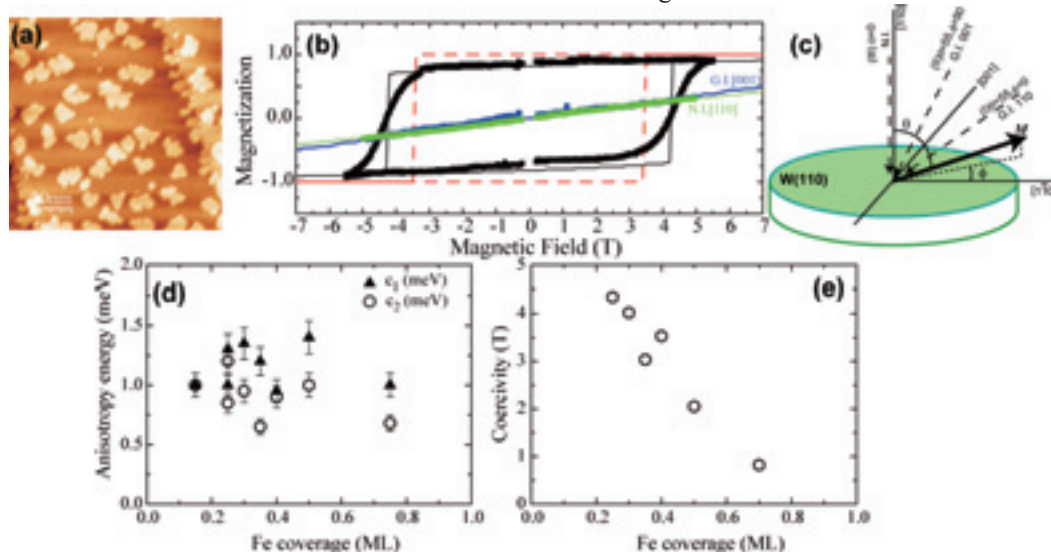
Molecular Orientation and Magnetic Properties of Vanadyl Phthalocyanine on Si(111)

K. Eguchi[1], Y. Takagi[1, 2], T. Nakagawa[1, 2] and T. Yokoyama[1, 2]

[1]*The Graduate University for Advanced Studies (SOKENDAI), Okazaki 444-8585, Japan*
[2]*Institute for Molecular Science, Okazaki 444-8585, Japan*

It is important to understand the interactions of phthalocyanine compounds containing transition metals (TMPcs) with semiconductor substrates as well as metal ones for realizing molecular devices. Vanadyl phthalocyanine (VOPc) is one of TMPcs formed non-planer structure although TMPcs (M=Mn, Fe, Co, Ni, Cu and Zn) are planar structure. For non-planar structure, it is possible to adsorb on substrates with oxygen pointing up or down in a case of adsorption parallel to the surface. Actually, VOPc in the first layer adsorbs on HOPG [1] and Au [2] substrates with oxygen pointing up and a GaAs substrate [3] with oxygen pointing down to the surface. In this study, we investigated the molecular orientation and magnetic properties of vanadyl phthalocyanine (VOPc) deposited on a clean Si(111)-(7×7) surface by using x-ray absorption spectroscopy (XAS) and x-ray magnetic circular dichroism (XMCD).

Purified VOPc was deposited on Si(111)-(7×7) from homemade Knudsen cell at 570K under 3×10^{-9} Torr. During the sublimation deposition, the substrate was kept at room temperature. The deposition rate estimated by a quartz crystal oscillator was 0.1 ML/min. XAS and XMCD measurements were performed at 5 K by means of total electron yield (TEY) detect. In the XMCD measurement, the helicity of the circularly polarized x-ray was fixed positively while the magnetic field was reversed.

Figure 1 shows the π^* resonance intensities of N K-edge x-ray absorption spectra for 0.9 and 15 ML VOPc deposited on clean Si(111) as a function of x-ray incident angle. It is found that the tilt angles of the phthalocyanine framework are about 26 deg and 37 deg for 0.9 ML and 15 ML VOPc, respectively. It is found that 15 ML VOPc does not form a molecular configuration with stand-up in comparison with a case of CuPc (β=66 deg) on Si(111) [4].

Figure 2 shows V L-edge and O K-edge XAS and XMCD spectra at the incident angle of 0 deg. The spectrum for 0.9 ML is broader than that for 15 ML because the energy resolution of the spectra for 0.9 ML was worse than that for 15 ML. However, it is clear that no additional peak is observed at V L-edge and the σ^* resonance intensity of O K-edge is increased for 0.9 ML VOPc as compared with that for 15 ML VOPc. It is found that VOPc molecules of the first layer on the surface are absorbed with oxygen pointing down to the surface and interacted chemically with Si atoms.

For the magnetic properties of VOPc films, XMCD signals are obtained for 0.9 ML VOPc as well as 15 ML VOPc. The XMCD spectra for both 0.9 ML and 15 ML are similar shape although the intensities are different. It is found that the electron of central vanadium atom in d-orbital does not be lost for 0.9 ML VOPc.
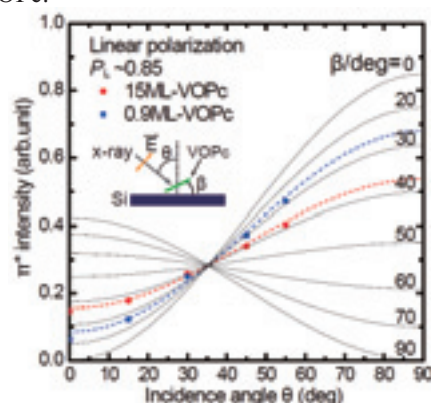

Fig. 1. The π^* resonance intensities are plotted as a function of the incident angle of x-ray with respect to the surface normal. The dashed lines are fitting curves.
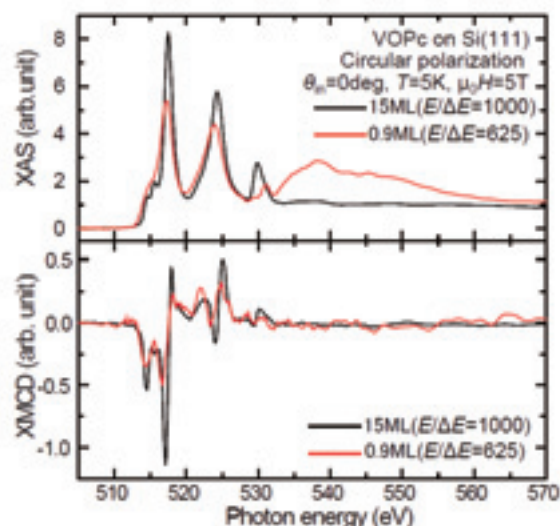

Fig. 2. V L-edge and O K-edge XAS and XMCD spectra for 0.9 and 15 ML VOPc/Si(111) taken at the incident angle of 0 deg from the surface normal at T=5 K and $\mu_0 H$=5 T.

[1] H. Fukagawa *et al.*, Phys. Rev. B **83** (2011) 085304.
[2] D.A. Duncan *et al.*, Surf. Sci. **604** (2010) 47.
[3] G. Mattioli *et al.*, J. Phys. Chem. Lett. **1** (2010) 2757.
[4] G. Dufour *et al.*, Surf. Sci. **319** (1994) 251.

Ⅲ-4. SURFACE AND THIN FILMS

Magnetic Property of Iron Phthalocyanine Absorbed on Nitrogen-Modified Cu(001) Surface

Y. Takagi[1, 2], K. Eguchi[2], T. Nakagawa[1, 2] and T. Yokoyama[1, 2]

[1] Institute for Molecular Science, Myodaiji-chio, Okazaki 444-8585, Japan
[2] The Graduate University for Advanced Studies, Okazaki, Aichi 444-8585, Japan

The magnetic properties of molecules have attracted interest in recent years. The spin states of the magnetic metal-complex molecules containing 3d transition metal can be changed by an adsorbed molecule and a substrate under the molecular films. Iron (II) phthalocyanine (FePc) is one of interesting and fundamental compounds, because it takes an unusual intermediate triplet spin state and has a large orbital moment. In this study, we report on the magnetic property of FePc on nitrogen saturated Cu(001) surface [Cu(001)-c(2x2)N] by means of X-ray magnetic circular dichroism (XMCD) at BL4B, which equipped with a super conducting magnet system.

Sample preparation and XMCD measurement were carried out in UHV chambers. A Cu(001) single crystal was cleaned by repeated cycles of Ar^+ sputtering and annealing. The N adsorbed surface was made by N^+ bombardment and annealing at 520 K. Purified FePc was deposited on the substrate at room temperature (RT) by sublimation and the thicknesses of the films were monitored by a quartz crystal oscillator. The X-ray absorption spectra (XAS) and XMCD spectra were taken at 5 K and the XMCD spectra were recorded with reversal of the magnetic field.

Figure 1 (a) shows Fe L-edge XMCD spectra of 25 ML FePc on clean Cu(001) and 1 ML FePc on Cu(001)-c(2x2)N at incident angle $\theta = 0^o$ from the surface normal at $H = \pm 5$ T. The spectra of FePc on Cu(001)-c(2x2)N is almost the same as that of 25 ML FePc. It seems that the inactivity of Cu(001)-c(2x2)N surface keep the same electronic state as FePc molecule in molecular plane. This result is different from the case of 1 ML FePc on the Co film [1]. The electronic state of FePc on Co films is modified by strong interaction between the FePc molecule and the Co layer.

In contrast to the result at $\theta = 0^o$, the spectrum of FePc film on Cu(001)-c(2x2)N at $\theta = 55^o$ is different from that of 25 ML FePc [Fig. 1 (b)]. The peak at 707 eV in FePc film on Cu(001)-c(2x2)N is weak compare with that in 25 ML FePc. The peak at 707 eV in XAS spectra originates from the $3d_{z^2}$ orbital of the Fe ion. Because the $3d_{z^2}$ orbital is oriented perpendicular to molecular plane, it is affected by the substrate under the molecule. Therefore, the decrease of the peak is caused by the interaction between the Fe $3d_{z^2}$ orbital and the Cu(001)-c(2x2)N substrate under the FePc molecule. These results indicate that the electronic state of

metal-complex molecules is modified only out of plane while that in in-plane is preserved the same electronic state of molecular.
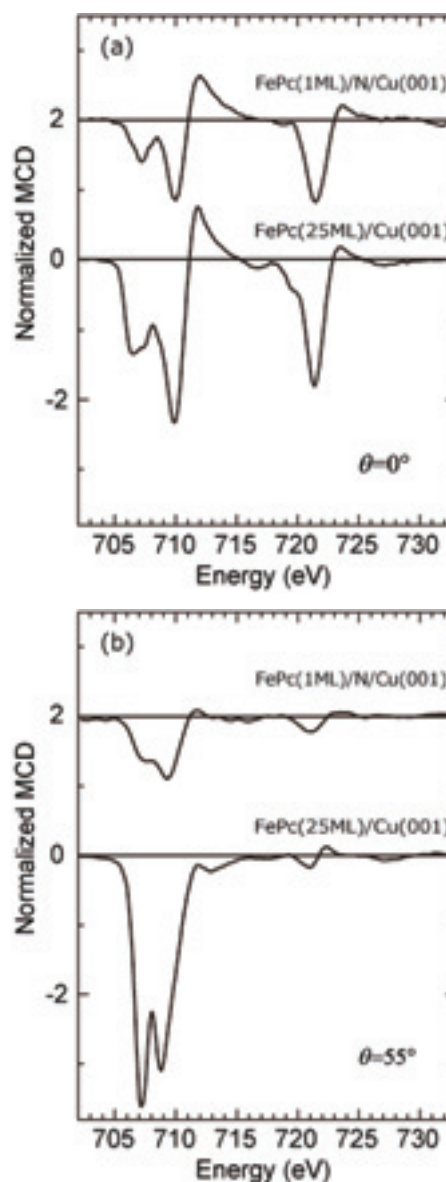

Fig. 1. Fe L-edge XMCD spectra of 25 ML FePc on clean Cu(001) and 1 ML FePc on Cu(001)-c(2x2)N at incident angle (a) $\theta = 0^o$, (b) $\theta = 55^o$ from the surface normal at $H = \pm 5$ T.

[1] Y. Takagi et al., UVSOR Activity Report **38** (2011) 67.

Novel Beam Splitter for High-Order Harmonics with WO$_3$/TiO$_2$ Bilayer Grown on c-Plane Sapphire Substrate

H. Kumagai[1], Y. Sanjo[1], M. Murata[1], Y. Nabekawa[2], K. Midorikawa[2], T. Shinagawa[3] and M. Chigane[3]

[1]*Graduate School of Engineering, Osaka City University, Osaka 558-8585, Japan*
[2]*RIKEN Advanced Science Institute, Wako, Saitama 351-0198, Japan*
[3]*Inorganic Materials Lab., Osaka Municipal Technical Research Institute, Osaka 536-8553, Japan*

High-intensity high-order harmonics have been investigated intensively in recent years. In the construction of a beam line for the high-intensity high-order harmonics, however, use of a conventional beam splitter (BS) (Si or SiC) that absorbs the fundamental laser light has caused serious problems such as its thermal distortion. To solve these problems, we proposed and investigated a novel BS with transparent oxide materials that transmitted the fundamental laser light and then reflected the high-order harmonics. In BS for the high-order harmonics, reflection of the fundamental laser light should be minimized by entering the p-polarized fundamental light at the Brewster's angle, which could improve the separation between the fundamental laser light and the high-order harmonics at the same Brewster's angle.

We have fabricated WO$_3$/TiO$_2$ bilayers on c-plane sapphire substrates by controlled growth with sequential surface chemical reactions (SSCR) using sequentially fast pressurized pulses of the vapor sources. Our previous experimental results revealed that WO$_3$ (221) and rutile TiO$_2$ (200) thin films could be grown epitaxially on c-plane sapphire substrates by SSCRs. Then, in this study, we proposed a WO$_3$/TiO$_2$ bilayer grown on c-plane sapphire substrates, which could be utilized as a BS for the high-order harmonics. Reflectance characteristics were also investigated at the same Brewster's angle using monochromatized synchrotron radiation (SR) located at Ultraviolet Synchrotron Radiation Facility (UVSOR), Institute for Molecular Science, Okazaki, Japan.

Reflectivities for x-rays were measured with the beamline BL5B at UVSOR, and the current from a Si photodiode was used to determine the beam intensity reflected from the fabricated BS. The reflectivity was obtained dividing the intensi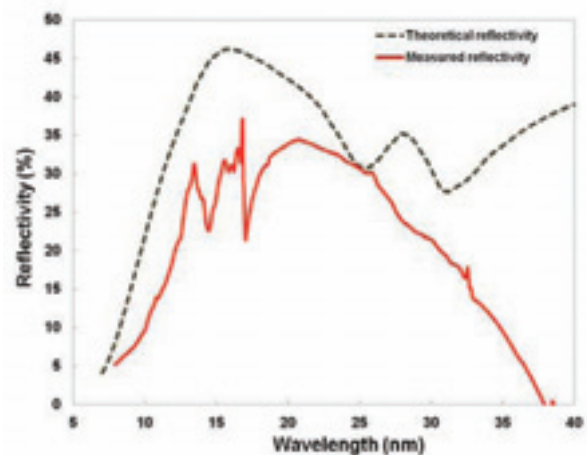ty of the reflected beam by that of the incident. Figure 1 shows theoretical (dashed line) and measured (solid line) reflectivities of WO$_3$/TiO$_2$/c-plane sapphire BS at the Brewster angle for TiO$_2$ at the pump pulse at the wavelength range from 7 nm to 40 nm. The measured peak reflectivity was 37.0% at a wavelength of approximately 16.8 nm, which corresponded to the 47th-order harmonics of the 800-nm pump pulse, while theoretical peak reflectivity was 45.2% at a wavelength of approximately 16.1 nm, which corresponded to the 49th-order harmonics of the

800-nm pump pulse. Figure 2 also shows high reflectivity of WO$_3$/TiO$_2$/c-plane sapphire BS at the Brewster angle for TiO$_2$ at the pump pulse at the wavelength range from 30 nm to 100 nm.

Fig. 1. Theoretical (dashed line) and measured (solid line) reflectivities of WO$_3$/TiO$_2$/c-plane sapphire BS at the Brewster angle for TiO$_2$ at the pump pulse at the wavelength range from 7 nm to 40 nm.
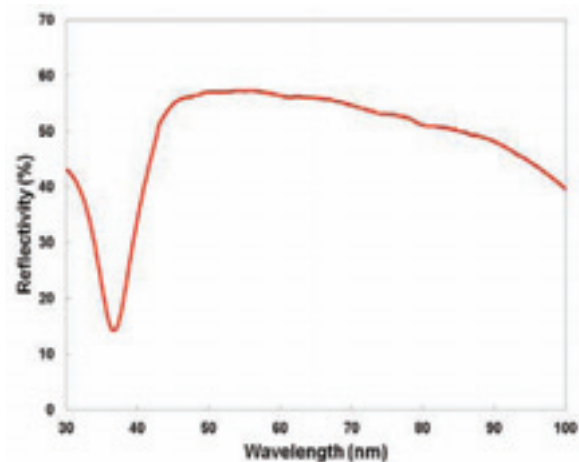

Fig. 2. Measured reflectivity of WO$_3$/TiO$_2$/c-plane sapphire BS at the Brewster angle for TiO$_2$ at the pump pulse at the wavelength range from 30 nm to 100 nm.

Ⅲ-4. SURFACE AND THIN FILMS

Characterization of Silicon Carbide Coated Concave Mirrors for Generation of Intense EUV FEL Fields

M. Fushitani, A. Matsuda, T. Endo and A. Hishikawa

Graduate School of Science, Nagoya University, Nagoya 464-8602, Japan

Thanks to advances in free electron laser (FEL) technology, a high power coherent light source has been recently available in the extreme ultraviolet (EUV) region. This new light source makes it possible to investigate nonlinear optical phenomena induced by intense EUV laser fields. When atoms interact with EUV FEL, they undergo multiphoton multiple ionization as a typical nonlinear response to the EUV laser fields, but details of the ionization mechanism have remained to be clarified. Recently, we have carried out photoelectron measurements with EUV FEL pulses at the SCSS facility of the RIKEN HARIMA institute, and have revealed importance of resonance effects in three-photon double ionization of Ar [1] as well as double excitation of He [2] in intense EUV laser fields, demonstrating that single-shot photoelectron spectroscopy is a powerful tool for studies of multiphoton multiple ionization. In these experiments, the FEL field intensity available by using the Kirkpatrick-Baez optics installed at the SCSS facility was an order of $\sim 10^{12}$ W/cm^2 due to the long focal length (~ 1 m), producing ions with at most doubly charged states. Therefore, to investigate the nonlinear response of atoms with highly charged states, mirrors with a high reflectivity as well as short focal length have to be employed for the focusing, thereby giving sufficiently large field intensities. Here, we investigate the reflectance property of a concave mirror ($f = 75$ mm) coated with silicon carbide (SiC) for the focusing of EUV FEL pules in the wavelength region of 50-61 nm.

The reflectance of a SiC coated concave mirror was measured at BL5B. The synchrotron radiation (SR) was dispersed by a grating and filtered in a confined region of 40-90 nm by a tin (Sn) foil (Fig. 1(a)) to suppress contributions from the higher order light due to the diffraction of the grating. The transmitted SR was detected at the normal angle by a Si photodiode (PD) suitable for the EUV region (AXUV100), which was used as a reference light. The SR light reflected by the SiC mirror at the angle of incidence of 7.5 degrees was measured with the same PD detector.

Figure 1 (b) shows a part of the reflectance of the SiC coated concave mirror. The reflectance increases from 40 nm and reaches the maximum of ~ 13 % around 65 nm. The wavelength region available for FEL at the SCSS facility is indicated by a double-headed arrrow. At 60 nm the reflectance is about 10 %, which is smaller than the throughput (30 %) of the focusing system at the SCSS, but the focal spot size of the SiC concave mirror is expected to be >10-times smaller. Therefore, based on comparisons of the focal areas, field intensities of EUV FEL pulses are expected to be improved by two orders of magnitudes, which results in intensities with an order of 10^{14} W/cm^2.

The present study strongly suggests that the SiC coated concave mirror with a short focal length is suitable for generating intense EUV laser fields with $\sim 10^{14}$ W/cm^2. Such large field intensities allow us to investigate how multiple ionization takes place to produce highly charged ions by using EUV FEL pulses.
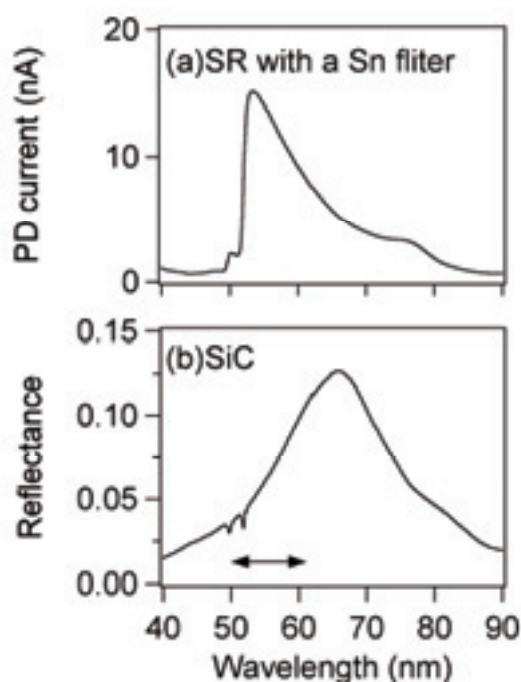
Fig. 1. (a) Synchrotron radiation dispersed by a grating and transmitted through a thin Sn filter, which is used as a reference light in the region of 40-90 nm. (b) Reflectance of a SiC coated concave mirror. The FEL wavelength region available at the SCSS facility is indicated by a double-headed arrrow.

[1] Y. Hikosaka *et al*., Phys. Rev. Lett. **105** (2010) 133001.
[2] A. Hishikawa *et al*., Phys. Rev. Lett. **107** (2011) 243003.

Charge Transfer from Methyelthiolate Monolayers on Metal Substrates Studied by Core Hole-Clock Spectroscopy

K. Nakaya[1], H. Yamane[2], M. Nagasaka[2], N. Kosugi[2] and H. Kondoh[1]

[1] *Graduate School of Science and technology, Keio University, Yokohama 223-8522, Japan*
[2] *Department of Photo-Molecular Science, Institute for Molecular Science, Okazaki 444-8585, Japan*

Organic molecules adsorbed on solid substrates are potentially useful for sensors and electronic devices. Charge transfer from the molecules to the substrate is one of key factors which determine the electronic property of such devices [1]. However, the relation between adsorption structure and charge transfer has been unclear. The core-hole clock spectroscopy is a powerful technique to estimate charge transfer time scale from molecule to substrate. The metal-thiolate bond is often used as a covalent-bond linker between organic moiety and substrate. In this work we studied charge transfer time scale of methylthiolate (CH_3S) adsorbed on Ag(111) and Cu(111), which exhibit largely different adsorption structures, using the core-hole clock spectroscopy.

The experiments were carried out at beamline BL6U of UVSOR. Ag(111) and Cu(111) surfaces were cleaned by Ar^+ ion spattering and annealing. The methylthiolate monolayers were prepared by evaporation of dimethyldisulfide (CH_3S-SCH_3) onto the metal substrates at room temperature. These samples were irradiated by soft x rays with photon energies of 220-245eV, and we measured intensities of electrons emitted in the decay process of S2s→3p excitation by an electron energy analyzer. Obtained S $L_1L_{2/3}M_{1/2/3}$ Coster-Kronig autoionization spectra exhibit delocalized and localized final states, where exited electrons are transferring to the substrate and remaining within the molecule, respectively. Comparison between the intensities of the two final states enables to estimate the charge-transfer time constant [2].

Figure 1 shows intensities as a function of incoming photon energy and kinetic energy of the emitted electrons taken for the methylthiolate monolayer on Cu(111). Four different final states appear on the spectra: delocalized final states with constant kinetic energies D ($2p^{-1}3p^{-1}deloc^1$) and d ($2p^{-1}3s^{-1}deloc^1$) and localized final states with linear dispersion L ($2p^{-1}3p^{-1}3p^1$) and l ($2p^{-1}3s^{-1}3p^1$). A single spectrum taken with a photon energy of 235.0 eV is shown in Fig. 2. The spectrum was de-convoluted into the four components to estimate the charge-transfer time constant. Since the L final state is contributed from another decay channel (shake-up photoionization), we used d and l components for the estimation. Referring the S 2s core-hole life time (τ_c=0.5 fs), the charge transfer time constant τ_{CT} was obtained using a simple equation $\tau_{CT} = \tau_c \times I(l)/I(d)$. As a result, $\tau_{CT}(Cu(111))$ is estimated to be 1.6 fs. In case of Ag(111), the component l was not clearly observed,

and hence the charge transfer for CH_3S/Ag(111) is extremely fast. Considering the previous result ($\tau_{CT}(Au(111))$ = 1.2 fs), it is concluded that $\tau_{CT}(Ag(111)) \ll \tau_{CT}(Au(111)) < \tau_{CT}(Cu(111))$.

In the CH_3S/Ag(111) system, the S atoms are buried in the Ag adatom layer, while in the case of Cu(111), CH_3S molecules are simply adsorbed on the surface. The CH_3S/Au(111) system shows formation of a surface complex consisting of a Au adatom and CH_3S. Therefore, the metal adatoms generated on the surface may play a significant role in formation of strong bonding between the S atom of methyelthiolate and the surface metal atoms, leading to faster charge transfer.
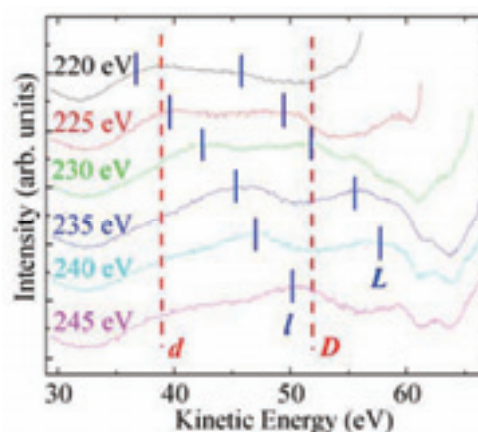

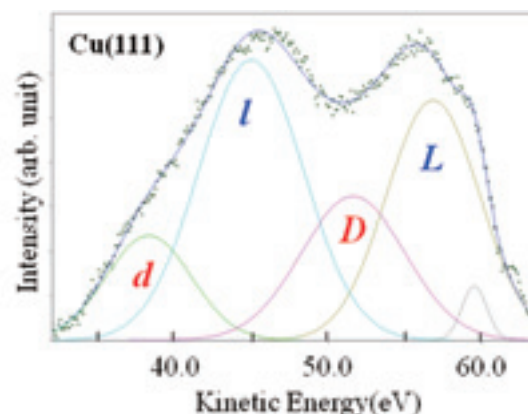Fig. 1. Intensities of the emitted electrons taken for the methylthiolate monolayer on Cu(111).

Fig. 2. Peak fitting of the spectrum at the photon energy of 235.0 eV.

[1] Li Wang, Wei Chen, Andrew Thye Shen Wee, Surf. Sci. Rep. **63** (2008) 465.
[2] A. Föhlisch *et al.,* Nature **436** (2005) 373.

Ⅲ-4. SURFACE AND THIN FILMS

Giant Rashba Spin-Orbit Splitting of Pt Nanowires on Silicon

S. W. Jung[1], S. H. Jeon[1], H. Yamane[2], N. Kosugi[2] and H. W. Yeom[1]

[1] Department of Physics and Center for Atomic Wires and Layers, Pohang University of Science and Technology, Pohang 790-784, Korea

[2] Department of Photo-Molecular Science, Institute for Molecular Science, Okazaki 444-8585, Japan

The Rashba effect is one of important physical mechanisms to realize spintronic devices, where the spin degeneracy of conduction channels is lifted without an external magnetic field [1,2]. This effect is caused by breaking space inversion symmetry at crystal surfaces. Recent researches found a few systems with very large Rashba effect [3,4,5], called giant Rashba splitting and revealed unusual spin textures of Rashba bands [3,4]. Moreover, an one-dimensional conductor formed on a silicon surface was found to exhibit Rashba spin splitting, which has a great potential in spintronics applications [8].

In the present study, we performed angle-resolved photoelectron spectroscopy (ARPES) measurements, using BL6U of UVSOR, for a newly found nanowire system formed on a silicon surface, Si (110)-"6"x5-Pt. This nanowire structure was previously studied by scanning tunneling microscopy (STM) [6]. As shown in Fig. 1, well ordered wires are formed along [1 -1 0] on the Si(110) substrate [6]. Our own STM study showed a x3 periodic structure on the bright part of the wires along [1 -1 0], which is mixed with a x2 periodic structure on the dark valleys between wires. Since this structure is formed with the heavy element Pt, we expected a substantial spin-orbit interaction on its band structure.

Figure 2 shows the ARPES data along [1 -1 0] direction taken at 15 K with 46 eV photon. Two parabolic bands (at binding energy of ~ 0.2 eV) are split at the Γ point with symmetric dispersions. This band was shown to have one-dimensional dispersion along the wires and its periodicity along the wires is consistent with that observed in STM. Its dispersion is further consistent with the Rashba splitting picture with a Rashba energy of about 130 meV and a Rashba parameter of about 0.93 eVÅ. This Rashba splitting is much larger than that on the two dimensional system of Si(111)-$\sqrt{3} \times \sqrt{3}$-Bi [5,7] or the one dimensional system of Si(557)-Au [8], belonging to the category of giant Rashba systems. The spin structure of this system needs to be further confirmed by spin-polarized ARPES experiments and the atomistic origin of the Rashba band needs to be clarified in the forthcoming works including theoretical calculation. In any case, we believe that this is the first one dimensional system with a giant Rashba effect.
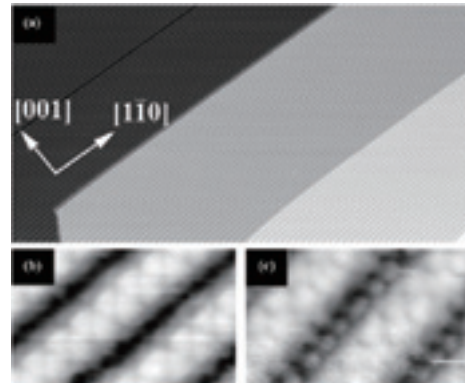

Fig. 1. STM topography of Si(110)-"6"x5-Pt taken from ref. [6]. (a) Wide region (300x150 nm^2 at filled state) and detailed images at (b) filled and (c) empty states.

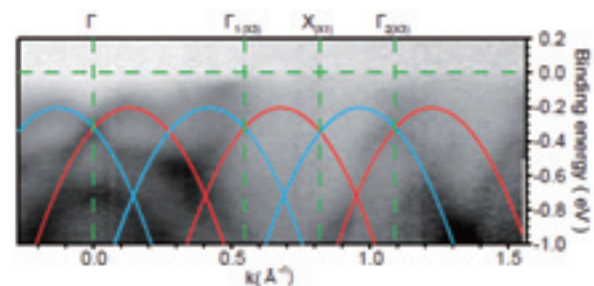Fig. 2. Measured band dispersion of Si(110)-"6"x5-Pt along the wire ([1 -1 0]) direction. Red and blue solid lines indicate the major surface state band dispersions, which show Rashba type band splitting.

[1] Y. A. Bychkov and E. I. Rashba, Journal of Physics C: Solid State Physics **17** (1984) 6039.
[2] E. I. Rashba, Journal of Superconductivity **15** (2002) 13.
[3] C. R. Ast *et al*., Phys. Rev. Lett. **98** (2009) 186807.
[4] K. Ishizaka *et al*. , Nat. Mater. **10** (2011) 521.
[5] I. Gierz *et al*. , Phys. Rev. Lett. **103** (2009) 046803.
[6] A. Visikovskiy, M. Yoshimura and K. Ueda, Appl. Surf. Sci. **254** (2008) 7626.
[7] K. Sakamoto *et al*. , Phys. Rev. Lett. **103** (2009) 156801.
[8] D. Sánchez-Portal, S. Riikonen and R. M. Martin, Phys. Rev. Lett. **93** (2004) 146803.

Warping Effects in the Band and Angular-Momentum Structures of the Topological Insulator Bi$_2$Te$_3$

W. S. Jung[1], Y. K. Kim[1], B. Y. Kim[1], Y. Y. Koh[1], Ch. Kim[1], M. Matsunami[2], S. Kimura[2], M. Arita[3], K. Shimada[3], J. H. Han[4], J. Kim[5], B. Cho[5] and C. Kim[1*]

[1]*Institute of Physics and Applied Physics, Yonsei University, Seoul, Korea*
[2]*UVSOR Facility, Institute for Molecular Science, Okazaki 444-8585 Japan*
[3]*HiSOR, Hiroshima University, Higashi-Hiroshima, Hiroshima 739-0046, Japan*
[4]*Department of Physics, Sungkyunkwan University, Suwon, Korea*
[5]*Department of Materials Science and Engineering, GIST, Gwangju 500-712, Korea*

The data from Bi$_2$Se$_3$ shows a large circular dichroism (CD), which stems from the existence of orbital angular momentum (OAM) [1]. It was found that the OAM is also locked to the electron momentum and its direction is antiparallel to the spin direction. Therefore, CD ARPES data may provide a way to measure the spin direction.

We report on our attempt to investigate the warping effect on the spin structures of the surface Dirac states of Bi$_2$Te$_3$ [2]. Our main goal was to obtain the systematic change in the OAM structure in the momentum space at a constant binding energy as a function of the energy from the Dirac point. Therefore, we performed ARPES experiments with circularly polarized light and obtained CD data. We observe the OAM direction from the dichroic ARPES data and find the spin structures. The results are consistent with the theoretical prediction, even in the high warping region.

To see how such a warping effect plays a role in the dichroism, we need to inspect the CD in the momentum space at a constant binding energy. Figure 1(b) plots constant energy CD data taken with 50 meV steps between 0 and 250 meV as marked by the dashed lines in Fig. 1(a). The plots show that the sign of the CD on a constant energy contour has binding energy dependence. Figure 1(c) shows CD data at 0, 100, and 250 meV binding energies. At 250 meV, which is close to the Dirac point, the shape of the constant energy contour is almost a circle. For 150 meV binding energy, the constant energy contour has a hexagonal shape. The Fermi contour at 0 meV binding energy has a strong warping effect, as manifested by its star shape. It is obvious that CD is also affected by the warping effect in Bi2Te3 and has a complex pattern.

CD plotted in Fig. 2 is very strong similar to CD results from Bi$_2$Se$_3$. We find that CD due to OAM is severely affected by the warping effect in the band structure. The OAM close to the Dirac point has an ideal chiral structure (sinθ) without the out-of-plane component. The CD shows a sin3θ effect in the weak warping effect region around 150 meV binding energy. Such θ dependence is compatible with the theoretically predicted spin structure for the case when the out-of-plane OAM component has a strong contribution to the θ dependence. In addition, CD

gets an extra sin6θ term from modulation in the in-plane OAM component when the warping effect becomes very strong near the Fermi energy. This result is consistent with theoretical prediction, which considers higher order terms in our modified *kp* perturbation theory that incorporates OAM.
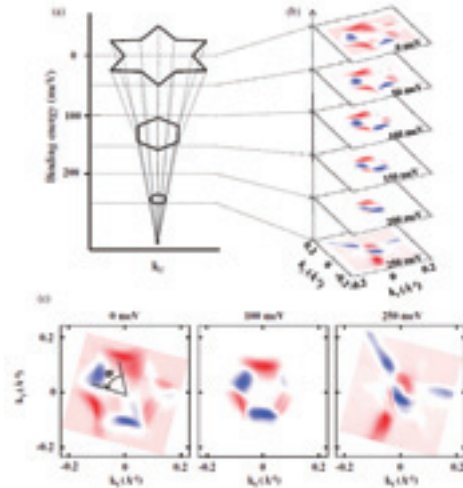

Fig. 1. (a) Illustration of Dirac cone of Bi$_2$Te$_3$. (b) Dichroism in the momentum space at various binding energies. (c) Constant dichroism map at selected binding energies of 0, 100, and 250 meV.
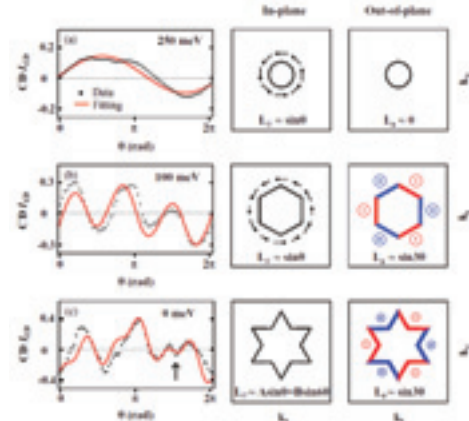

Fig. 2. CD and OAM direction along the constant energy contour at (a) 0 meV, (b) 100 meV, and (c) 250 meV.

[1] S. R. Park *et al.,* Phys. Rev. Lett. **108** (2012) 046805.
[2] W. Jung *et al.,* Phys. Rev. B **84** (2011) 245435.

Ⅲ-4. SURFACE AND THIN FILMS

Reflection Spectroscopy of KTa$_{1-x}$Nb$_x$O$_3$ Thin Films by Reactive Sputtering

T. Goto, K. Nishimura, A. Yuasa, T. Tanaka and H. Matsumoto

School of Science & Technology, Meiji University, Kawasaki 214-8571, Japan

KTN (KTa$_{1-x}$Nb$_x$O$_3$) is a transparent optical crystal that is made of K, Ta, Nb, and O and exists as amorphous, pyrochlore, and perovskite crystal structures. Interestingly, it does not undergo a structural phase transition below its melting point temperature [1]. Furthermore, KTN having a perovskite crystal structure exhibits a very large electro-optic effect, wherein the refractive index changes by twice the magnitude of the applied voltage. The purpose of this study was to achieve optical responses for KTN thin film over a wide range of photon energies, and to investigate the electronic structures by comparing experimental data with theoretical calculations.

Thin films of KTa$_{1-x}$Nb$_x$O$_3$ ($0 \leq x \leq 0.7$) were deposited by radio frequency (RF) reactive sputtering onto fused quartz at a temperature of 500 °C. KTaO$_3$ and Nb plates were used as the target, and the sputtering was conducted in a mixture of argon and oxygen gases. The film thickness was about 150 nm. The chemical bonding states and crystallinity of the films were investigated by X-ray photoelectron spectroscopy (XPS) and X-ray diffraction (XRD) analyses. Reflection spectra of the films were measured in the vacuum ultraviolet region up to 40 eV with a 3 m normal incidence monochromator (gratings: G1, G2, and G3) using the BL7B beamline at UVSOR-II. A silicon photodiode sensor was used as the detector for the reflected light.

According to the analyses, all thin films are composed of polycrystalline KTN. When the impression electric power of Nb was measured at 0, 25, 50, 100, and 125 W, the value of x was set to 0, 0.10, 0.16, 0.47, and 0.59, respectively. The reflective measurement results using the beamline at UVSOR are shown in Fig. 1. As the value of x increased, the peaks at 5 eV and 10 eV shifted to the low energy side. To analyze the differences, a DV-Xα molecular orbital calculation was performed. The calculation results and the experimental measurements are in good agreement. The results of the calculation are shown in Figs 2 and 3, which are the energy level diagrams of [M$_7$K$_8$O$_{36}$] (M = Ta, Nb) clusters embedded in Madelung potential is represented by the formal charges. In each oxide, the O$_{2p}$ band comprises the valence band. The calculation results show that the peak shifts as x increases is the peak for the Nb$_{4d}$ orbital.

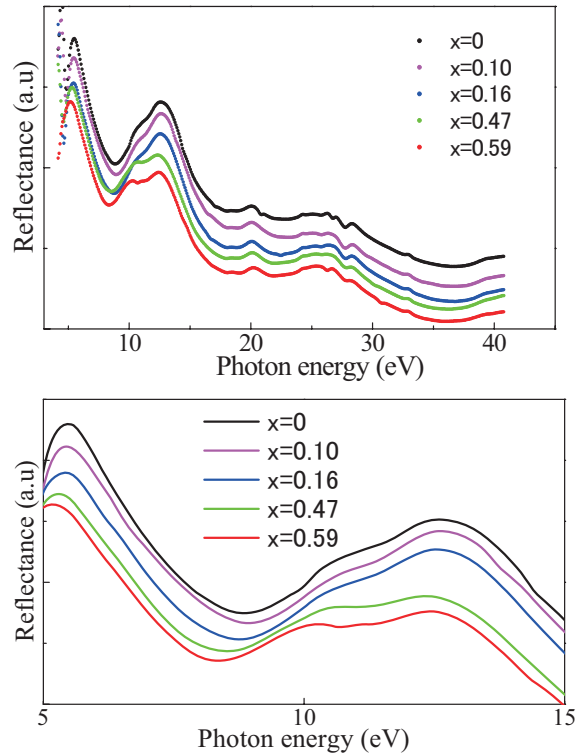[1] C. J. Lu , A. X. Kuang , G. Y. Huang and S. M. Wang , J. Materials Science **31** (1996) 3081.

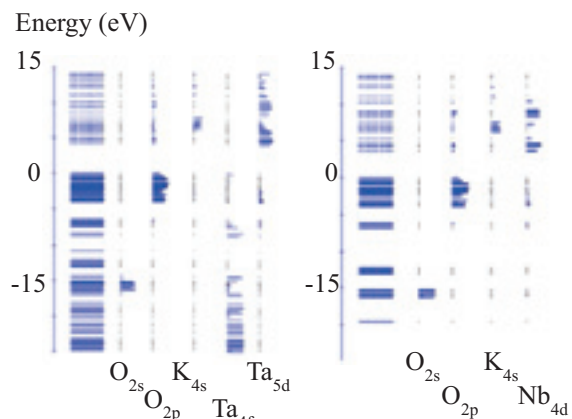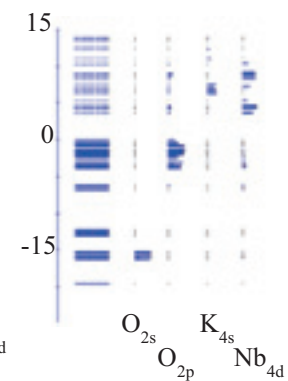Fig. 1. Measurement results using the BL7B beamline at UVSOR

Fig. 2. KTaO$_3$ Fig. 3. KNbO$_3$

Interface Electronic Structure of Diindenoperylene on Ag(111)

S. Kera[1], T. Hosokai[2], R. Kamiya[2], A. Gerlach[3] and N. Ueno[1]

[1]*Graduate School of Advanced Integration Science, Chiba University, Chiba 263-8522, Japan*
[2]*Faculty of Engineering, Iwate University, Morioka 020-8551, Japan*
[3]*Institut für Angewandte Physik, Universität Tübingen, Tübingen 72076, Germany*

Over the past decade, organic electronic devices have increased considerable attentions due to their potential applications. The adsorption of large π-conjugated organic molecules on metal surfaces is one of the key targets to understand the variety of peculiar interface properties. The molecule-substrate interaction crucially influences electronic and geometric properties at the interface.

Diindenoperylene (DIP: $C_{32}H_{16}$) (inset in Figure 1) is a typical organic semiconductor. The DIP monolayer films are prepared on graphite (HOPG) and Ag(111) substrate to reveal the interface electronic structure by using angle-resolved ultraviolet photoelectron spectroscopy (ARUPS).

ARUPS spectra were measured at photon incidence angle α=45°, hv=28 and 40 eV and T=295 K. The molecules were evaporated onto the graphite and Ag(111). The coverage/thickness of the monolayer was confirmed by the work function of the densely-packed monolayer (ML) film which shows a clear LEED pattern.

Figure 1 shows the UPS of DIP thin films on Ag(111) together with DIP monolayer (ML) on HOPG for the comparison. The DIP/HOPG spectrum (4) can be considered for the representative of physisorbed interface. The peaks A, B and C are ascribed to HOMO(π), HOMO-1(π) and HOMO-2(π), respectively. These valence features are appeared at high-binding energy (E_b) side by 0.35eV for DIP/Ag(111) (3). The peaks are suppressed and shifted to low-E_b side with decreasing the coverage. For the thinner films, the additional features are observed especially at band-gap region, which is denoted by $I_1 - I_3$. One may find other valence band features at around peak I_3 and at deeper E_b region, though it is hard to discuss the characteristics of each state due to coexistence a couple of orbital states. The features I_1 and I_2 would be related to the former LUMO and former HOMO of DIP as reported similarly in PTCDA/Ag(111), respectively [1]. Shockley surface state is completely disappeared for the film (1). The work function of the DIP(ML)/Ag(111) is decreased by 0.44 eV from Ag(111) and slightly recovered for other thicker films (2) and (3) by 0.1eV. The spectrum (1) is also obtained upon annealing the thicker films.

Figure 2 shows ARUPS result for DIP(ML)/Ag(111) along Γ−K direction measured at hv=28 eV. The photoelectron angular distributions (PADs) of features I_1 and I_2 are slightly different each other. The PAD for molecular solids gives a momentum view of molecular orbital spread [2]. To reveal each orbital character beyond the energy resolution, a momentum map of the PAD is requested to be measured [3]. The adsorption distance evaluated by x-ray standing wave measurements remarks a closer distance for DIP than PTCDA on Ag(111). The relation between the adsorption distance and the degree of orbital hybridization to the metal, which may be appeared in the present UPS results, will be considered.

[1] J. Ziroff *et al.,* Phys. Rev. Lett. **104** (2010) 233004.
[2] S. Kera *et al.*, Chem. Phys. **325** (2006) 113.
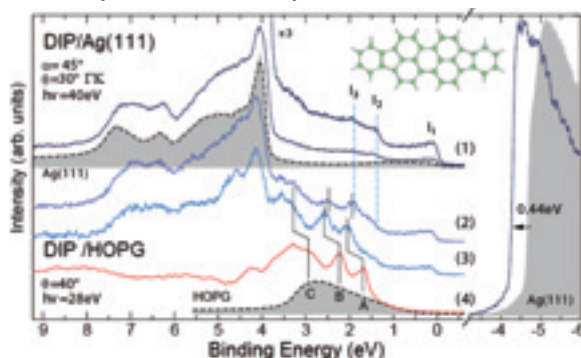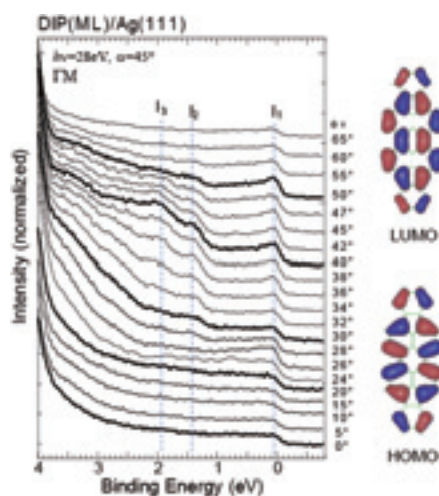[3] M. Dauth *et al*., Phys. Rev. Lett. **107** (2011) 193002.

Fig. 1. Thickness dependence of DIP film prepared on a clean Ag(111), DIP(as-grown ML: 0.3 nm) (1), DIP(island film 0.6 nm) (2), and DIP(1 nm) (3) together with DIP(as-grown ML)/HOPG (4). UPS for each substrate are also shown. Work function shift (0.44 eV) is found for the secondary cut-off region.

Fig. 2. ARUPS along Γ−K direction for DIP(as-grown ML)/Ag(111). HOMO and LUMO distribution on gas-phase are also shown.

ARUPS Study of Anisotropic Molecular Orientation of Pentacene Thin Film on Microstructured Substrate

K. K. Okudaira, T. Ishii, K.Hotta and N. Ueno

Association of Graduate Schools of Science and Technology, Chiba Univererity, Chiba 263-8522, Japan

Recent progress in the field of organic thin-film transistors receives significant attention underscoring its importance for the microelectronic industry. In organic electronic devices, the electrical behavior is governed by not only the electronic states of the semiconducting molecules but also the morphology of their thin films. In-plane orientation of pentacene films has been performed in order to improve the transport properties in OFETs. Fabrication of oriented structure such as uniaxially oriented crystallites is important to obtain the oriented growth of materials as a substrate. In-plane orientation of pentacene films has been performed in order to improve the transport properties in OFETs. Fabrication of oriented structure such as uniaxially oriented crystallites is important to obtain the oriented growth of materials as a substrate. It has been shown that the uniaxially film growth of pentacene can be achieved by using micrsotructured substrate. In this study we show that a highly anisotropic growth of pentacene film on the uniaxially oriented poly (tetrafluoroethylene) (PTFE) onto the grating which have well-defined microstructure (such as groove period and depth).

ARUPS measurements were performed at the beamline BL8B of the UVSOR storage ring at the Institute for Molecular Science. The take-off angle (θ) dependencies of photoelectron spectra were measured at incident angle of photon (α) = 45° with the photon energy (hν) of 40 eV. All measurements were performed at room temperature. PTFE was deposited on brazed grating with different groove period (300line/mm (line space is 3.3 μm) and 1200 line/mm (line space is 830 nm) on which Cu has been deposited in advance. Pentacene thin film was obtained by deposition on PTFE film onto the grating (Pn/PTFE/grating).

We observed take-off angle (θ) dependence of HOMO peak in UPS of pentacene thin film (thickness of about 10 nm) on PTFE film deposited on grating Pn/PTFE/grating (300 lines/mm) and (1200 lines/mm) with parallel and perpendicular condition [Fig.1(a) and (b)]. In the parallel condition, the electrical vector of incidence photon is parallel to the direction of the groove. Photoelectron intensities from HOMO band show a sharp θ dependence with a maximum at θ = 50~60°. On the contrary, with parallel condition they show broader θ dependence. θ dependence for the pentacene thin film on grating (1200 lines/mm) is sharper than that on grating (300 lines/mm). They indicate that the anisotropy of molecular orientation of pentacene on the grating (1200 lines/mm) is higher than that on the grating

(300 lines/mm). The narrower line space (below 800 nm) needs for the higher anisotropic molecular orientation of pentacene film.
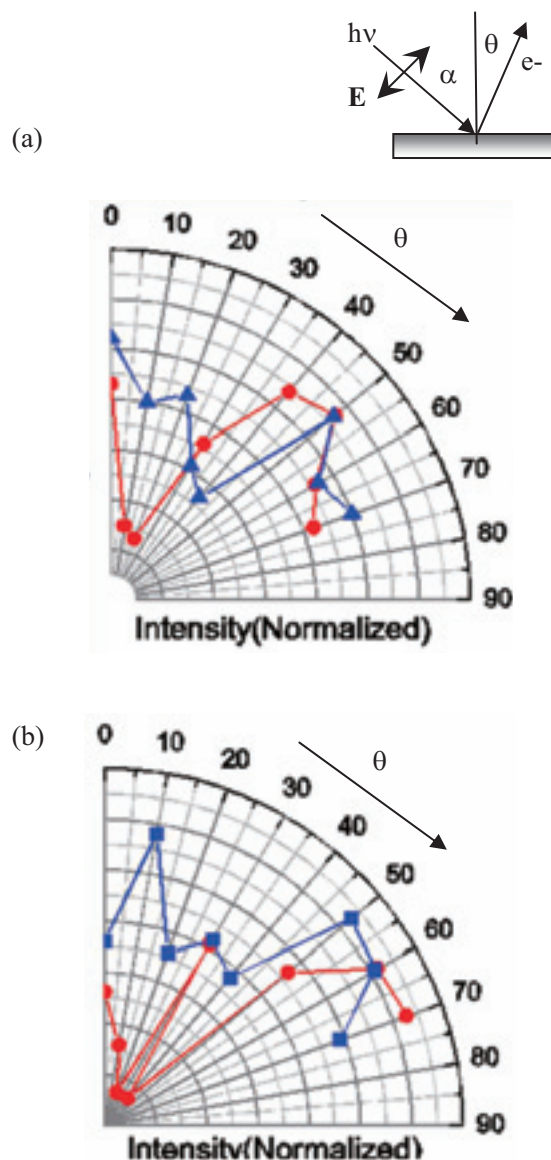

Fig.1. Take-off angle (θ) dependences of photoelectron intensities of HOMO peak of Pn/PTFE/grating (300 lines/mm) (a) and Pn/PTFE/grating (1200 lines/mm) (b) with parallel (●) and perpendicular condition (●).